Investigating the environmental interpretation of oxygen and carbon isotope data from whole and fragmented bivalve shells

Lacey, J.H.[1]*, Leng M.J.[1,2,] Peckover, E.N.[3], Dean, J.R.[4], Wilke, T.[5], Francke, A.[6,7], Zhang, X.[8], Masi, A.[9], Wagner, B.[6]

[1] NERC Isotope Geosciences Facilities, British Geological Survey, Keyworth, Nottingham, UK

[2] Centre for Environmental Geochemistry, School of Biosciences, Sutton Bonington Campus, University of Nottingham, Loughborough, UK

[3] School of Environmental Sciences, University of East Anglia, Norwich, UK

[4] School of Environmental Sciences, University of Hull, Hull, UK

[5] Department of Animal Ecology & Systematics, Justus Liebig University Giessen, Giessen, Germany

[6] Institute of Geology and Mineralogy, University of Cologne, Cologne, Germany

[7] School of Earth and Environmental Science, University of Wollongong, Wollongong, Australia

[8] Institute of Loess Plateau, Shanxi University, Taiyuan, China

[9] Department of Environmental Biology, Sapienza University, Rome, Italy

*corresponding author

Keywords: Holocene; Palaeoclimate; Stable isotopes; Bivalvia; *Dreissena carinata*; Shell fragments; Lake sediment; Lake Dojran

Abstract

Sclerochronological data from whole bivalve shells have been used extensively to derive palaeoenvironmental information. However, little is known about the relevance of shell fragments more commonly preserved in the sediment record. Here, we investigate the oxygen and carbon isotope composition of *Dreissena carinata* fragments from a core recovered from Lake Dojran (FYRO Macedonia/Greece) to identify their relevance and efficacy as a proxy in palaeoenvironmental studies. We use a modern *Dreissena* shell to calibrate the relationship between the bivalve and its contemporary environment, which suggests their isotope composition is primarily a function of temperature and water balance. The range of fragment isotope data from the core overlaps with that of unbroken fossil shells, suggesting the fragments broadly record lakewater conditions across the time of deposition. A comparison of the isotope composition of shell fragments and endogenic carbonate shows an offset between the two sets of data, which is likely due to temperature differences between surface and bottom waters, the timing of carbonate precipitation, and productivity-controlled stratification of the dissolved inorganic carbon pool. Shell fragment isotope data seem to reflect the signal of environmental change recorded in other proxy data from the same core and may potentially be used (like endogenic carbonate) to provide information on past changes in lake level.

1 Introduction

The isotope composition of carbonate from the sequential analysis of intact fossil bivalves is being increasingly utilised in palaeoenvironmental reconstructions (Schöll-Barna et al., 2012; Lewis et al., 2017). However, little is known about the relevance of the isotope composition of shell fragments, which are commonly preserved in the sedimentary record (Wagner et al., 2014; Marcano et al., 2015). To better understand the efficacy of shell fragments as proxy in

palaeoenvironmental studies, we utilise sediment cores recovered from Lake Dojran (Balkan Peninsula) that have been previously investigated using multi-proxy techniques and contain both whole shells and fragments of the bivalve *Dreissena carinata*.

The bivalve genus *Dreissena* is renowned for including two of the most invasive of all freshwater organisms, *Dreissena polymorpha* and *Dreissena rostriformis*, but also comprises species restricted to their native distribution (Albrecht et al., 2007). Lake Dojran is thought to exclusively contain *D. carinata* (Wilke et al., 2010). Although information on the ecological tolerances of *D. carinata* is limited, they will be similar to *D. polymorpha* as the two species have a close phylogenetic relationship. *Dreissena* spp. typically live for 2-19 years and their shells are characterised by external rings that form when growth slows or stops due to changes in environmental conditions (e.g. temperature, water depth, trophic conditions, current strength, turbidity; Karatayev et al., 2006). Shell growth typically starts at ~10 °C and if temperatures exceed ~32 °C most mussels die (Karatayev et al., 2006). Within Lake Dojran, young *D. carinata* are mainly found on the littoral lakebed and adults typically occur attached to sublittoral hard substrates, such as empty shells and pebbles, and often form small clusters (Šapkarev, 1980; Griffiths et al., 2002; our observations).

The oxygen isotope composition ($\delta^{18}O$) of bivalve carbonate (typically aragonite) is a function of the temperature and $\delta^{18}O$ of lakewater ($\delta^{18}O_{lake}$; Leng and Marshall, 2004; Goewert et al., 2007), assuming isotopic equilibrium and no diagenetic alteration, as there are limited vital effects on $\delta^{18}O$ in freshwater bivalves (Dettman et al., 1999; Geist et al., 2005). Equilibrium precipitation of biogenic aragonite is subject to a temperature-dependent fractionation between the carbonate and water, where $\delta^{18}O$ decreases by 0.23 ‰ for every +1°C (Grossman and Ku, 1986; Dettman et al., 1999). The carbon isotope composition ($\delta^{13}C$) of bivalves typically reflects the $\delta^{13}C$ of the dissolved inorganic carbon pool (DIC), where any disequilibrium between the shell and DIC is relatively constant (Apolinarska, 2013).

Consequently, changes in $\delta^{18}O_{lake}$, $\delta^{13}C_{DIC}$, and temperature will be recorded in subsequent layers of the shell during growth.

Here we test the potential of using the isotope composition of bivalve shell fragments in palaeoenvironmental studies by investigating: 1) how $\delta^{18}O$ and $\delta^{13}C$ of modern whole *D. carinata* shells relates to present day lakewater, 2) if shell fragments from sediment cores reflect the isotope range of fossil whole shells, and 3) the relationship between shell $\delta^{18}O$ and $\delta^{13}C$ and other proxy data. We provide a modern calibration using stable isotope data from a recent shell and monitoring data from Lake Dojran, and present sequential isotope data from whole shells from the early Holocene. The fossil whole shell data are combined with isotope data from shell fragments, which occur in variable quantities through the Holocene, and are compared with previous palaeoenvironmental investigations on the same core sequence.

2 Study site

Lake Dojran (41°12'N, 22°44'E; 144 m asl) is located on the border between the Former Yugoslav Republic of Macedonia and Greece (Figure 1) in an elliptical karst basin of Neogene age. The lake is 8.9 km long and 7.1 km wide. The lake has a volume of 0.3 km^3 with gently inclined slopes, a surface area of 42 km^2, and an average water depth of 6.5 m (Francke et al., 2013). Water inflow is primarily derived from small rivers, creeks, and groundwater sourced from precipitation over the catchment. Outflow is dominated by summer evaporation, and also via groundwater, irrigation, and water supply to local populations (Gesovska, 2016). The lake has no natural outflow, however, during times of higher lake level, the River Doiranitis connects Dojran to the Vardar River and the Aegean Sea (Sotiria and Petkovski, 2004). The lake is monomictic, experiencing thermal stratification in summer months, with overturn likely occurring during winter (Temponeras et al., 2000; Zacharias et al., 2002; Lokoska et al., 2006). The lakewater is eutrophic with a pH of 7.6-9.5,

an electrical conductivity of 0.8-1.5 mS/cm (Sotiria and Petkovski, 2004) and total phosphorous of 50-520 µ/L (measured during 2004-2006; Tasevska et al., 2012).

The climate of the local area is characterised by hot and dry summers and mild, humid winters (Popovska et al., 2005). Temperature and precipitation are influenced by Aegean Sea through the Thessaloniki Plain and continental influences from the north. The average air temperature is 14.3 °C, ranging between 26.1 °C and 3.7 °C, and annual precipitation is 630 mm (Sotiria and Petkovski, 2004; Popovska et al., 2005). The mean weighted annual isotope composition of precipitation has $\delta^{18}O = -7.4$ ‰ and $\delta D = -48$ ‰, ranging between −10.6 ‰ in winter and −3.2 ‰ in summer for $\delta^{18}O$ (calculated on-line at waterisotopes.org; Bowen et al., 2005). Inflow $\delta^{18}O$ plots close to the Global Meteoric Water Line (GMWL; Craig, 1961), whereas $\delta^{18}O_{lake}$ defines a local evaporation line (LEL; Figure 2). Therefore, $\delta^{18}O_{lake}$ is controlled primarily by the water balance of the lake (Leng and Marshall, 2004), for example a decrease in $\delta^{18}O_{lake}$ of −2.9 ‰ between 1997 and 2011 coincided with a lake level increase of ~4 m (Griffiths et al., 2002; Francke et al., 2013). Spring inflows have $\delta^{13}C_{DIC}$ between −13.0 ‰ and −7.9 ‰, which is lower than lakewater values of between −5.9 ‰ and −0.6 ‰ (Figure 2; Griffiths et al., 2002; Francke et al., 2013). There is negligible impact from geological carbonate within the basin and $\delta^{13}C_{DIC}$ is mainly influenced by in-lake processes, such as exchange with atmospheric CO_2 and/or the preferential uptake of ^{12}C by algae during photosynthesis (Leng and Marshall, 2004).

3 Material and methods

A ~7 m sediment core (Co1260; Figure 1) was recovered in June 2011 using gravity and percussion piston corers from a site of undisturbed, horizontally-bedded sediments (water depth = 6.6 m). Cores were recovered in 3 m-long sections, cut to 1 m, and then split

lengthways and subsampled continuously at 2 cm intervals (a full overview of coring, sampling, sedimentology, and chronology is described in Francke et al. (2013)).

Subsamples were sieved (63 µm) to separate larger shelly material from fine-grained clays and endogenic carbonate. Intact shells were rare in the subsamples. Alongside a modern shell collected from the littoral zone in June 2011 (Figure 3), two fossil shells from 447.9 cm and 470.9 cm core depth were recovered and appeared well preserved. The whole shells were sampled sequentially along the ridge of the shell from the umbo to ventral margin using a Dremel rotary hand drill with a 1 mm bit, which produced a fine powder. Fragmented shells occurred in varying proportions throughout the core (Figure 3). Only those subsamples which contained at least five individual fragments between 0.5-1 mm (sizeable enough to provide >50 µg of carbonate) were selected for isotope analysis. Individual fragments were crushed to a fine powder prior to analysis. Scanning electron microscopy (SEM) with energy dispersive X-ray spectroscopy (EDX), X-ray Diffraction (XRD), and X-ray fluorescence (XRF) were used to confirm that the dominant carbonate species forming the shell material is aragonite, with no evidence of calcite.

Stable isotope analysis was conducted at the British Geological Survey. Approximately 50-200 µg of powder was analysed using an Isoprime dual inlet mass spectrometer coupled to a Multiprep device, by reaction with concentrated phosphoric acid for 15 minutes at 90°C. Carbon and oxygen isotope values for the whole shells ($\delta^{13}C_{shell}$ and $\delta^{18}O_{shell}$) and shell fragments ($\delta^{13}C_{frag}$ and $\delta^{18}O_{frag}$) are reported as parts per mil (‰) calculated to the Vienna Pee Dee Belemnite (VPDB) scale using a within-run laboratory standard (KCM) calibrated to international NBS standards. Analytical reproducibility for KCM was <0.1 ‰ for both $\delta^{13}C$ and $\delta^{18}O$. The mineral-gas fractionation factor used for aragonite was 1.00854 (derived from Kim et al., 2007a).

4 Results

The modern shell (24.9 mm long) has average $\delta^{18}O_{shell}$ = −0.3 ± 1.0 ‰ (1σ), ranging between +2.3 ‰ and −1.3 ‰, and average $\delta^{13}C_{shell}$ = −1.7 ± 1.0 ‰ (1σ), ranging between +0.3 ‰ and −3.4 ‰ (Figure 4). There is a strong correlation between $\delta^{18}O_{shell}$ and $\delta^{13}C_{shell}$ (r = +0.8, p < 0.005, n = 24). The fossil shell from 447.9 cm (9.5 cal kyr BP; 14.7 mm long) has average $\delta^{18}O_{shell}$ = −0.7 ± 0.9 ‰ (1σ), ranging between +1.2 ‰ and −2.5 ‰, and average $\delta^{13}C_{shell}$ = −1.5 ± 0.8 ‰ (1σ), ranging between −0.2 ‰ and −2.8 ‰ (Figure 4). A strong covariation is present between $\delta^{18}O_{shell}$ and $\delta^{13}C_{shell}$ (r = +0.9, p < 0.005, n = 15). The fossil shell from 470.9 cm (10.0 cal kyr BP; 22.4 mm long) has average $\delta^{18}O_{shell}$ = −2.1 ± 0.8 ‰ (1σ), ranging between −0.7 ‰ and −3.3 ‰, and average $\delta^{13}C_{shell}$ = −1.7 ± 0.6 ‰ (1σ), ranging between −0.8 ‰ and −2.7 ‰ (Figure 4). There is a strong covariation between $\delta^{18}O_{shell}$ and $\delta^{13}C_{shell}$ (r = +0.8, p < 0.005, n = 21).

Overall, the fragments have average $\delta^{18}O_{frag}$ = −0.2 ± 1.2 ‰ (1σ) and $\delta^{13}C_{frag}$ = −2.2 ± 1.1 ‰ (1σ), ranging between +3.1 and −3.9 ‰ and +0.5 and −4.9 ‰, respectively (Figure 5). Individual horizons have ranges of 1.1 to 5.4 ‰ for $\delta^{18}O_{frag}$ and 0.7 to 4.2 ‰ for $\delta^{13}C_{frag}$. There is a moderate covariation between $\delta^{18}O_{frag}$ and $\delta^{13}C_{frag}$ for the whole sequence (r = +0.6, p < 0.005, n = 119), however late Holocene fragments show a stronger covariation (r = +0.8, p < 0.005, n = 80) whereas early Holocene-Younger Dryas fragments do not have a significant correlation (r = +0.3, p = 0.06, n = 39).

5 Discussion

5.1 $\delta^{18}O$ and $\delta^{13}C$ of whole shells

The modern whole shell contained soft body remains, which suggests the animal died directly (a few days) before collection in June 2011. The geochemistry of the shell's ventral margin should therefore represent lakewater conditions at this time, assuming growth until death. The

ventral margin has $\delta^{18}O_{shell}$ = +1.07 ‰ and, using $\delta^{18}O_{lake}$ = −0.91 ‰ (Francke et al., 2013) with the equation of Grossman and Ku (1986), the calculated lakewater temperature was ~11°C. The only thermal gradient data for the lake are from 1996 when water depth was ~5 m, which give 1°C/m during summer and 2-3°C/m in spring and autumn (Temponeras et al., 2000). As the gradient would have been greater in 2011 when water depth was ~7 m, the calculated ~11°C for bottom waters is consistent with surface temperatures of ~24°C in May-June (Temponeras et al., 2000). This infers that precipitation was most likely in equilibrium with lakewater, as for other bivalves (Goewert et al., 2007). Further, shell growth was probably not continuous throughout the year as temperatures would be too low between early autumn and late spring (Karatayev et al., 2006).

The modern shell shows decreasing $\delta^{18}O$ and $\delta^{13}C$ from the umbo, followed by an increase toward the ventral margin (Figure 4). The shell presumably represents ~8 years of growth given its length (Karatayev et al., 2006), which covers a period of major lake level change. Between 1988 and 2002, lake level decreased by ~5 m following water extraction for irrigation (Griffiths et al., 2002), before levels increased after a remediation project diverted water into the lake (Gesovska, 2016). Inflow to the lake has low $\delta^{18}O$ (−8 ‰; Francke et al., 2013), and therefore greater input would decrease $\delta^{18}O_{lake}$. In addition, air temperature was ~1 °C lower than present during the main phase of lake level rise (Gesovska, 2016), and evaporation would have been marginally reduced also lowering $\delta^{18}O_{lake}$. However, these effects will have been counteracted by a higher lake level resulting in a larger surface area and increased evaporation (Francke et al., 2013). A higher thermal gradient would also reduce bottom water temperature driving higher $\delta^{18}O_{shell}$. Any direct influence of temperature change on the fractionation between aragonite and lakewater would have been countered by an inversely proportional change in regional rainfall $\delta^{18}O$ (Bard et al., 2002). Therefore, greater inflow with low $\delta^{18}O$ must have outweighed the net effects of evaporation,

temperature, and thermal gradient changes to result in the transition to low $\delta^{18}O_{shell}$. Lake level was then stable between 2006 and 2009 whilst average air temperature increased by ~2 °C (Gesovska, 2016). This probably led to stronger evaporation and higher $\delta^{18}O_{lake}$, supported by a larger surface area and greater evaporation potential, and a higher thermal gradient and lower bottom water temperatures. Rising lake level and lower temperatures toward the end of the bivalve's life would account for lower $\delta^{18}O_{shell}$ at the ventral margin.

A strong covariation between $\delta^{18}O_{shell}$ and $\delta^{13}C_{shell}$ ($r = 0.8$, $p = <0.001$, $n = 24$) suggests that periods of low $\delta^{18}O_{lake}$ are associated with low $\delta^{13}C_{DIC}$. Inflow $\delta^{13}C$ is lower than lakewater $\delta^{13}C_{DIC}$ (Francke et al., 2013), therefore greater inflow will lead to lower $\delta^{18}O_{lake}$ and $\delta^{13}C_{DIC}$. In addition, higher inflow could dilute nutrient levels, reducing aquatic productivity and limiting the export of ^{12}C from lakewaters, also leading to lower $\delta^{13}C_{DIC}$. Periods of higher temperature and evaporation would increase atmospheric exchange, driving higher $\delta^{13}C_{DIC}$ and covariation between $\delta^{18}O$ and $\delta^{13}C$ (Talbot, 1990; Leng and Marshall, 2004). As with the modern shell, there is a strong covariance between $\delta^{18}O$ and $\delta^{13}C$ in the whole shells from 447.9 and 470.9 cm core depth ($r = \geq 0.8$, $p = <0.001$). The fossil shells show larger variations in $\delta^{18}O$ and $\delta^{13}C$ than the modern shell (i.e. saw-tooth profile), which may be due to changes in growth rate, length of growing season, or greater seasonality. The pattern of variability is most likely consistent with the interpretation of the modern shell, where lower $\delta^{18}O_{lake}$ and $\delta^{13}C_{DIC}$ are driven by increased inflow and higher values by evaporative processes. On a seasonal basis, the delivery of water with low $\delta^{18}O$ and $\delta^{13}C_{DIC}$ occurs during colder winter months, whereas less inflow and higher evaporation is characteristic of warmer summer months.

5.2 $\delta^{18}O$ and $\delta^{13}C$ of shell fragments

Bivalves produce superior reinforcement in the direction of shell growth, which means shells preferentially fracture along concentric growth surfaces that represent planes of structural weakness (Böhm et al., 2016). Each fragment consists of multiple growth bands (Figure 3), and therefore may represent up to several years of growth. As the fragments could not be sub-sampled, any environmental signal will be averaged. While each individual fragment may span a few years, collectively they are presumably the remains of littoral shell beds and therefore provide a relatively low-resolution indicator of environmental change. Larger fragments were more abundant in sections of the core that broadly coincide with a higher sedimentation rate, which are associated with periods of lower lake level (Francke et al., 2013; Zhang et al., 2014; Masi et al., 2017). These periods may have been characterised by a higher energy environment capable of moving the fragments from the littoral zone to the coring location, which would also promote faster burial rates and reduce the potential for reworking. The overriding presence of small shell fragments within fine-grained sediments suggests the fragments have been transported and are not in situ as part of a palaeoshoreline. This is corroborated by seismic data showing only flat-lying sediments at the coring location (Francke et al., 2013) and by the fragments being sub-angular with rounded edges (Figure 3). This morphology suggests the original fracturing could have been due to biogenic breakage, which typically produces straight-edged fragments, and indicates abrasion during breakage and/or transport.

The fragments will be subject to a residence time before final deposition, and each sampling horizon will contain fragments originating from different individuals. As core sampling was carried out at every 2 cm, the majority of sampling horizons represent ~14-46 years, depending on sedimentation rate. This technique is consequently appropriate for establishing

interdecadal changes in environmental conditions, although information from individual growing seasons could potentially be derived from sub-sampling individual fragments.

To establish the effectiveness of utilising shell fragments in palaeoenvironmental reconstructions, the fragment isotope data were compared to fossil whole shell data from nearby core horizons. The range in $\delta^{18}O_{shell}$ and $\delta^{13}C_{shell}$ partially overlaps the range in $\delta^{18}O_{frag}$ and $\delta^{13}C_{frag}$ at core intervals around 10 cal kyr BP and 9.5 cal kyr BP (Figure 5). Any offset is most likely due to a variable $\delta^{18}O_{frag}$ and $\delta^{13}C_{frag}$ range between sampling horizons, where the range in $\delta^{18}O_{frag}$ is 1.1 to 5.4 ‰ (average = 2.6 ‰) and 0.7 to 4.2 ‰ for $\delta^{13}C_{frag}$ (average = 2.2 ‰). Although range differences between levels could be due to changes in seasonality, the variability is more likely a function of sampling limitations. This may include only capturing a limited range of climate variability from the available fragments, differential reworking after deposition (e.g. bioturbation), or using shells from different microenvironments within the lake. However, the average $\delta^{18}O_{frag}$ and $\delta^{13}C_{frag}$ range is similar to that observed for $\delta^{18}O_{shell}$ and $\delta^{13}C_{shell}$ (2.6 to 3.7 ‰ and 1.9 to 3.7 ‰, respectively) suggesting that the fragment range approximates average lakewater conditions for the time of deposition. As with the modern shell, the fossil whole shells and fragments will have formed predominantly through warmer months of the year when higher temperatures promoted growth. Therefore, these data should be comparable to variations in the isotope composition of endogenic carbonate ($\delta^{18}O_{carb}$ and $\delta^{13}C_{carb}$) from the lake that precipitates in surface waters as calcite (Francke et al., 2013).

5.3 Comparison with multi-proxy data from Co1260

Comparing the fragment and calcite data, average $\delta^{18}O_{frag}$ is higher than $\delta^{18}O_{carb}$ (+1.7 ‰) and $\delta^{13}C_{frag}$ is lower than $\delta^{13}C_{carb}$ (–3.0 ‰; Figure 5). Although part of the $\delta^{18}O$ offset is due to the positive fractionation between aragonite and calcite (~ +0.8 ‰; Kim et al., 2007b), a

difference is still present after taking this into account (average $\delta^{18}O_{frag}$ = –0.2 ‰ and $\delta^{18}O_{carb}$ = –1.9 ‰). An offset to lower $\delta^{18}O_{carb}$ may indicate calcite formed early in the year when $\delta^{18}O_{lake}$ is lower after winter recharge or during warmer months where high temperatures would give lower $\delta^{18}O_{carb}$ (Leng and Marshall, 2004). As calcite precipitation is driven by productivity and higher surface temperatures (Francke et al., 2013), temperature control on $\delta^{18}O_{carb}$ will likely produce the offset from $\delta^{18}O_{frag}$. In addition, due to the temperature gradient, calcite will form in the epilimnion at higher temperatures than the bivalve aragonite on the lakebed, which forces higher $\delta^{18}O_{shell}$. Bivalve growth also most likely starts at ~10 °C in spring, continues through summer when calcite is precipitated, and slows/stops in autumn where $\delta^{18}O_{lake}$ will be higher due to summer evaporation.

The offset between average $\delta^{13}C_{frag}$ and $\delta^{13}C_{carb}$ (–3.0 ‰) may be related to productivity differences between surface and bottom waters, with strong productivity driving calcite precipitation and removing ^{12}C resulting in higher $\delta^{13}C_{DIC}$ in the epilimnion. Any recycling of the sinking organic matter may result in lower $\delta^{13}C_{DIC}$ in bottom waters. A difference in $\delta^{13}C_{DIC}$ between surface and bottom waters would also be enhanced by thermal stratification during summer (Zacharias et al., 2002).

As for $\delta^{18}O_{frag}$, an extended growth period will expose shells to a range of $\delta^{13}C_{DIC}$, particularly in the early and later parts of the year when recharge delivers water with low $\delta^{13}C_{DIC}$ (Francke et al., 2013). $\delta^{13}C_{frag}$ and $\delta^{13}C_{carb}$ broadly trace similar trends through the Holocene, taking into account the low resolution of shell data. These correspond to variations in $\delta^{13}C$ of organic matter ($\delta^{13}C_{org}$; Figure 5), for example a shift to lower $\delta^{13}C$ between ~10 and 7 cal kyr BP and a change to higher $\delta^{13}C$ in the late Holocene (although calcite is absent). As average $\delta^{13}C_{org}$ is −25.5 ‰ and $\delta^{13}C_{DIC}$ = −5.9 ‰ (in 2011; Francke et al., 2013), organic matter is likely autochthonous as phytoplankton typically have $\delta^{13}C$ that is 20 ‰ lower than

$\delta^{13}C_{DIC}$ (Meyers, 2003). Further, this indicates that variations in $\delta^{13}C_{frag}$, $\delta^{13}C_{carb}$, and $\delta^{13}C_{org}$ are a function of changes in $\delta^{13}C_{DIC}$.

The trend to lower $\delta^{13}C$ starting around 10 cal kyr BP traces increasing arboreal pollen (AP), particularly mesophilous plants, and higher reconstructed temperatures (Masi et al., 2017; Thienemann et al., 2017). Increasing water depth and higher trophic levels are also indicated by a shift to a plankton-dominated diatom assemblage (Figure 5; Zhang et al., 2014). A change to lower $\delta^{13}C$ under higher trophic levels suggests $\delta^{13}C_{DIC}$ is likely a function of increasing catchment soil development (higher AP; Masi et al., 2017; Rothacker et al., 2018), and the delivery of respired soil CO_2 with low $\delta^{13}C$ (as suggested for nearby Lake Ohrid; Lacey et al., 2015). A gap in shell fragment data (7.7-2.7 cal kyr BP) is probably due to a high lake level increasing the distance from coring location to the shore, thereby reducing the focussing of shell material and widening the non-habitable zone in the central basin due to a finer substrate. In the late Holocene, a lower lake level is suggested by fewer planktonic diatoms (Zhang et al., 2014), and is consistent with lower temperatures and a regional shift to drier conditions (Roberts et al., 2008; Thienemann et al., 2017). A change to higher $\delta^{13}C$ is likely due to reduced water input (less soil CO_2 inflow) and a lower precipitation to evaporation ratio, both driving higher $\delta^{13}C_{DIC}$. This is also evident in the modern lake. Under lower lake level in 1997 $\delta^{13}C_{DIC}$ = +0.2 ‰ compared to −5.9 ‰ in 2011 under a higher lake level (Figure 2; Griffiths et al., 2002; Francke et al., 2013), although the time of sampling (June vs. September) may account for part of the difference.

The degree of offset between $\delta^{18}O_{frag}$ and $\delta^{18}O_{carb}$ may provide additional information on lake level changes. Around 9.6 cal kyr BP, there is little difference between average $\delta^{18}O_{frag}$ and $\delta^{18}O_{carb}$ (+0.3 ‰) and average $\delta^{18}O_{shell}$ overlaps with $\delta^{18}O_{carb}$ (Figure 5). The early Holocene is characterised by a rise in benthic diatom taxa suggesting a low lake level under higher temperatures (Figure 5; Zhang et al., 2014; Thienemann et al., 2017), which would reduce the

lakewater temperature gradient and result in a smaller offset between $\delta^{18}O_{frag}$ and $\delta^{18}O_{carb}$. At ~8 cal kyr BP there is a larger offset of ~ +2 ‰. This is associated with a diatom-inferred lake level rise (Zhang et al., 2014), which would increase the temperature gradient and drive higher $\delta^{18}O_{frag}$ thereby forcing a decoupling with $\delta^{18}O_{carb}$.

6 Conclusions

Shell carbonate most likely precipitates in isotopic equilibrium with lakewater through part of the year as low temperatures limit growth over winter into spring. $\delta^{18}O$ and $\delta^{13}C$ are suggested to be primarily influenced by shifts in lake level and water balance, which in turn effect the lakewater temperature gradient and DIC pool. Breakage patterns indicate that shells preferentially fragment along growth surfaces. As fragments originate from multiple individuals over an extended period, $\delta^{18}O_{frag}$ and $\delta^{13}C_{frag}$ most likely represent average interannual-decadal environmental conditions. As $\delta^{18}O_{frag}$ and $\delta^{13}C_{frag}$ broadly correspond to the ranges obtained in continuous profiles from fossil whole shells, this suggests that the fragments represent average lakewater conditions during sedimentation. An offset between the isotope composition of shells and calcite is most likely controlled by temperature variations during precipitation associated with lake level changes ($\delta^{18}O$) and soil development in the catchment ($\delta^{13}C$). Downcore variations in the offset between the $\delta^{18}O$ of shell fragments and calcite may indicate changes in lake level. Our data suggest that shell fragment $\delta^{18}O$ and $\delta^{13}C$ can provide useful palaeoenvironmental information, in particular as part of a multiproxy study and where endogenic carbonate is absent.

7 Acknowledgements

JL, ML, JD, and EP prepared the manuscript, with support from all authors. The project was started by EP as part of an MGeol at the University of Leicester. EP undertook the majority

of the lab work, supervised by ML. We thank Nick Marsh, Cheryl Haidon, and Rob Wilson (University of Leicester), and Hilary Sloane and Paul Witney (BGS) for technical support.

8 References

Albrecht, C., Schultheiß, R., Kevrekidis, T., Streit, B., Wilke, T., 2007. Invaders or endemics? Molecular phylogenetics, biogeography and systematics of *Dreissena* in the Balkans. Freshwater Biology 52, 1525-1536.

Bard, E., Delaygue, G., Rostek, F., Antonioli, F., Silenzi, S., and Schrag, D. P., 2002. Hydrological conditions over the western Mediterranean basin during the deposition of the cold Sapropel 6 (ca. 175 kyr BP). Earth and Planetary Science Letters 202, 481-494.

Böhm, C.F., Demmert, B., Harris, J., Fey, T., Marin, F., Wolf, S.E., 2016. Structural commonalities and deviations in the hierarchical organization of crossed-lamellar shells: A case study on the shell of the bivalve *Glycymeris glycymeris*. Journal of Materials Research 31, 536-546.

Bowen, G.J., Wassenaar, L.I., Hobson, K.A., 2005. Global application of stable hydrogen and oxygen isotopes to wildlife forensics. Oecologia 143, 337-348.

Craig, H., 1961. Isotopic variations in meteoric waters. Science 133, 1833–1834.

Dettman, D.L., Reische, A.K., Lohmann, K.C., 1999. Controls on the stable isotope composition of seasonal growth bands in aragonitic fresh-water bivalves (*Unionidae*). Geochimica et Cosmochimica Acta 63, 1049-1057.

Francke, A., Wagner, B., Leng, M.J., Rethemeyer, J., 2013. A Late Glacial to Holocene record of environmental change from Lake Dojran (Macedonia, Greece). Climate of the Past 9, 481-498.

Geist, J., Auerswald, K., Boom, A., 2005. Stable carbon isotopes in freshwater mussel shells: Environmental record or marker for metabolic activity? Geochimica et Cosmochimica Acta 69, 3545-3554.

Gesovska, V., 2016. Water Balance Model of Vulnerability Assessment of Dojran Lake Basin. International Journal of Advanced Research in Science, Engineering and Technology 3, 1942-1951.

Goewert, A., Surge, D., Carpenter, S.J., Downing, J., 2007. Oxygen and carbon isotope ratios of Lampsilis cardium (*Unionidae*) from two streams in agricultural watersheds of Iowa, USA. Palaeogeography, Palaeoclimatology, Palaeoecology 252, 637-648.

Griffiths, H.I., Reed, J.M., Leng, M.J., Ryana, S., Petkovskic, S., 2002. The recent palaeoecology and conservation status of Balkan Lake Dojran. Biological Conservation 104, 35-49.

Grossman, E.L., Ku, T.L., 1986. Oxygen and carbon isotope fractionation in biogenic aragonite: temperature effects. Chemical Geology 59, 59-74.

Karatayev, A.Y., Burlakova, L.E., Padilla, D.K., 2006. Growth rate and longevity of *Dreissena polymorpha* (Pallas): A review and recommendations for future study. Journal of Shellfish Research 25, 23-32.

Kim, S.-T., Mucci, A., Taylor, B.E., 2007a. Phosphoric acid fractionation factors for calcite and aragonite between 25 and 75 °C: Revisited. Chemical Geology 246, 135-146.

Kim, S.-T., O'Neil, J.R., Hillaire-Marcel, C., Mucci, A., 2007b. Oxygen isotope fractionation between synthetic aragonite and water: Influence of temperature and Mg2+ concentration. Geochimica et Cosmochimica Acta 71, 4704-4715.

Lacey, J.H., Francke, A., Leng, M.J., Vane, C.H., Wagner, B., 2015. A high-resolution Late Glacial to Holocene record of environmental change in the Mediterranean from Lake Ohrid (Macedonia/Albania). International Journal of Earth Sciences 104, 1623-1638.

Leng, M.J., Marshall, J.D., 2004. Palaeoclimate interpretation of stable isotope data from lake sediment archives. Quaternary Science Reviews 23, 811-831.

Lewis, J.P., Leng, M.J., Dean, J.R., Marciniak, A., Bar-Yosef Mayer, D.E., Wu, X., 2017. Early Holocene palaeoseasonality inferred from the stable isotope composition of *Unio* shells from Çatalhöyük, Turkey. Environmental Archaeology 22, 79-95.

Lokoska, L., Jordanoski, M., Veljanoska-Sarafiloska, E., Tasevska, O., 2006. Water quality of Lake Dojran from biological and physical chemical aspects. In: BALWOIS 2006, Ohrid.

Marcano, M.C., Frank, T.D., Mukasa, S.B., Lohmann, K.C., Taviani, M., 2015. Diagenetic incorporation of Sr into aragonitic bivalve shells: implications for chronostratigraphic and palaeoenvironmental interpretations. The Depositional Record 1, 38-52.

Masi, A., Francke, A., Pepe, C., Thienemann, M., Wagner, B., and Sadori, L., 2017. Vegetation history and palaeoclimate at Lake Dojran (FYROM/Greece) during the Late Glacial and Holocene. Climate of the Past Discussions, https://doi.org/10.5194/cp-2017-114, accepted.

Meyers, P.A., 2003. Applications of organic geochemistry to palaeolimnological reconstructions: a summary of examples from the Laurentian Great Lakes. Organic Geochemistry, 34, 261-28.

Popovska, C., Gesovska, V., Ivanoski, D., 2005. Ecological and hydrological state of Dojran Lake. Vodoprivreda 37, 175-180.

Roberts, N., Jones, M.D., Benkaddour, A., Eastwood, W.J., Filippi, M.L., Frogley, M.R., Lamb, H.F., Leng, M.J., Reed, J.M., Stein, M., Stevens, L., Valero-Garcés, B., Zanchetta, G., 2008. Stable isotope records of Late Quaternary climate and hydrology from Mediterranean lakes: the ISOMED synthesis. Quaternary Science Reviews 27, 2426-2441.

Rothacker, L., Dosseto, A., Francke, A., Chivas, A.R., Vigier, N., Kotarba-Morley, A.M., Menozzi, D., 2018. Impact of climate change and human activity on soil landscapes over the past 12,300 years. Scientific Reports 8, 1-7.

Rubinson, M., Clayton, R.N., 1969. Carbon-13 fractionation between aragonite and calcite. Geochimica et Cosmochimica Acta 33, 997-1002.

Šapkarev, J., 1980. Composition and variation of bottom fauna in the sublittoral of the eutrophic Lake Dojran (Macedonia, Yugoslavia). Developments in Hydrobiology 3, 195-201.

Schöll-Barna, G., Demény, A., Serlegi, G., Fábián, S., Sümegi, P., Fórizs, I., Bajnóczi, B., 2012. Climatic variability in the Late Copper Age: stable isotope fluctuation of prehistoric *Unio pictorum* (*Unionidae*) shells from Lake Balaton (Hungary). Journal of Paleolimnology 47, 87-100.

Sotiria, K., Petkovski, S., 2004. Lake Doiran – An overview of the current situation. Greek Biotope/Wetland Centre (EKBY), Society for the Investigation and Conservation of Biodiversity and the Sustainable Development of Natural Ecosystems (BIOECO), Thermi.

Talbot, M.R., 1990. A review of the palaeohydrological interpretation of carbon and oxygen isotopic ratios in primary lacustrine carbonates. Chemical Geology: Isotope Geoscience section 80, 261-279.

Tasevska, O., Jersabek, C.D., Kostoski, G., Gušeska, D., 2012. Differences in rotifer communities in two freshwater bodies of different trophic degree (Lake Ohrid and Lake Dojran, Macedonia). Biologia 67, 565-572.

Temponeras, M., Kristiansen, J., Moustaka-Gouni, M., 2000. Seasonal variation in phytoplankton composition and physical-chemical features of the shallow lake Doirani, Macedonia, Greece. Hydrobiologia 424, 109-122.

Thienemann, M., Masi, A., Kusch, S., Sadori, L., John, S., Francke, A., Wagner, B., Rethemeyer, J., 2017. Organic geochemical and palynological evidence for Holocene natural and anthropogenic environmental change at Lake Dojran (Macedonia/Greece). The Holocene, 27, 1103-1114.

Wagner, B., Leng, M.J., Wilke, T., Böhm, A., Panagiotopoulos, K., Vogel, H., Lacey, J.H., Zanchetta, G., Sulpizio, R., 2014. Distinct lake level lowstand in Lake Prespa (SE Europe) at the time of the 74 (75) ka Toba eruption. Climate of the Past 10, 261-267.

Wilke, T., Schultheiß, R., Albrecht, C., Bornmann, N., Trajanovski, S., Kevrekidis, T., 2010. Native *Dreissena* freshwater mussels in the Balkans: in and out of ancient lakes. Biogeosciences 7, 3051-3065.

Zacharias, I., Bertachas, I., Skoulikidis, N., Koussouris, T., 2002. Greek Lakes: Limnological overview. Lakes & Reservoirs: Research and Management 7, 55-62.

Zhang, X., Reed, J., Wagner, B., Francke, A., Levkov, Z., 2014. Lateglacial and Holocene climate and environmental change in the northeastern Mediterranean region: diatom evidence from Lake Dojran (Republic of Macedonia/Greece). Quaternary Science Reviews 103, 51-66.

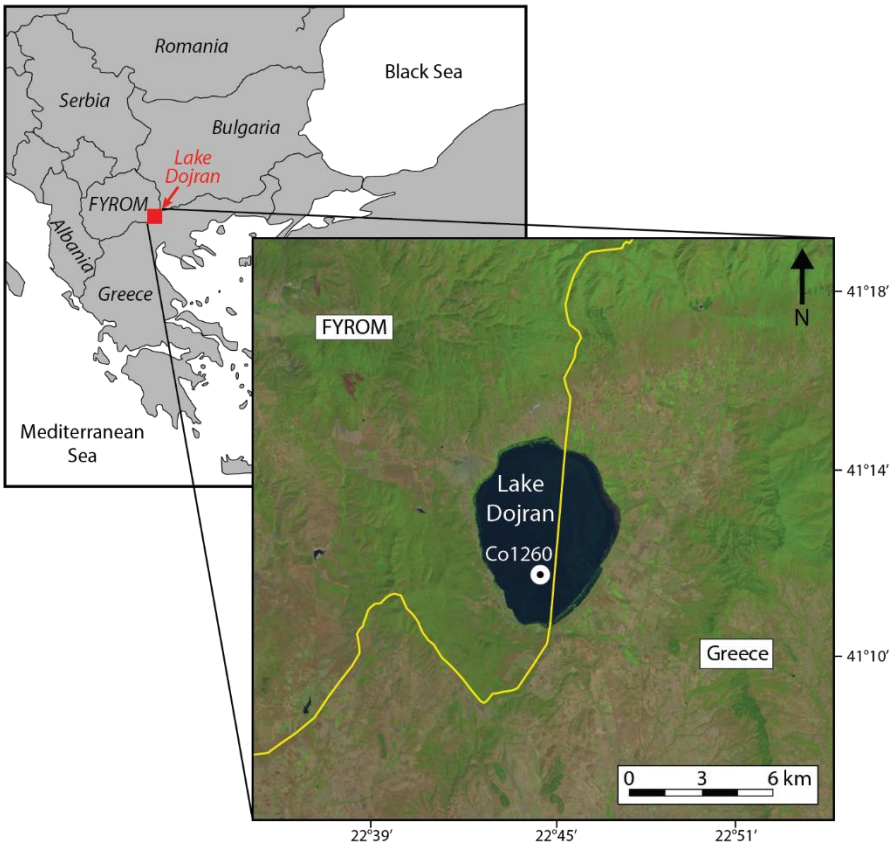

Figure 1 Map of the Balkan Peninsula showing the location of Lake Dojran on the border between the Former Yugoslav Republic of Macedonia and Greece, and the location of Co1260.

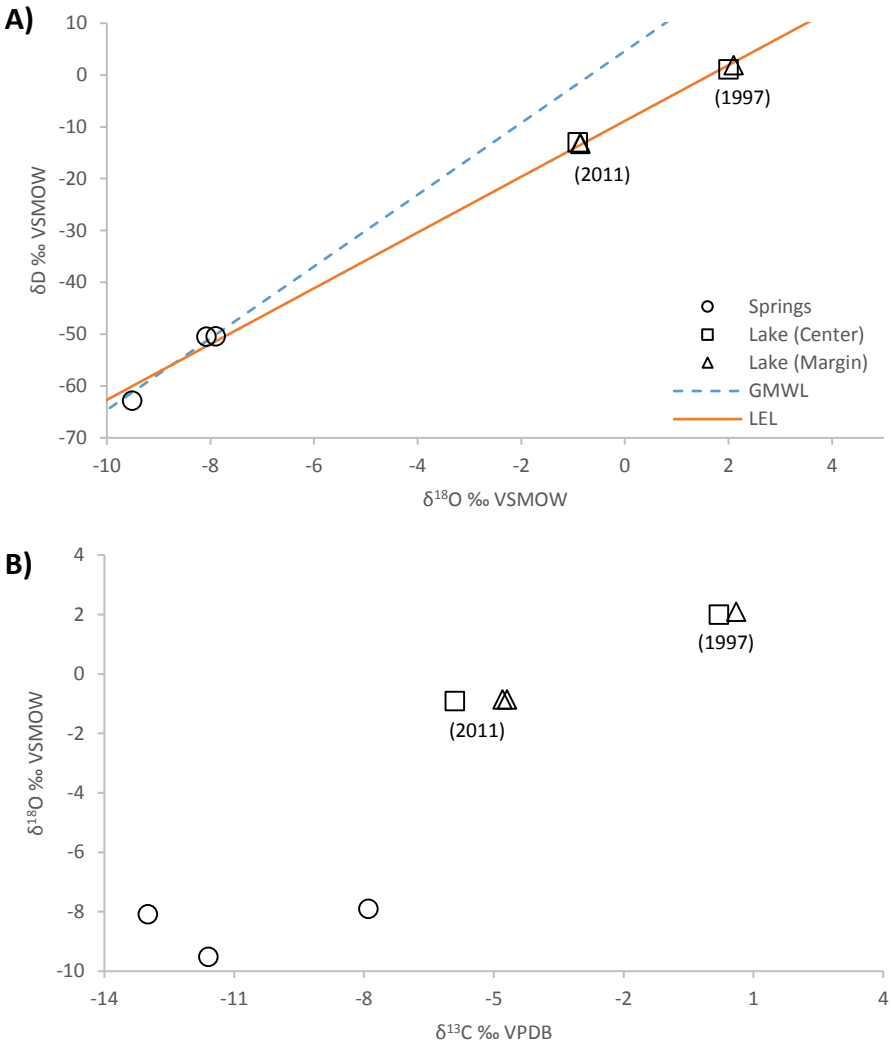

Figure 2 Stable isotope composition of (A) lake water and spring inflows ($\delta^{18}O$ and δD; Griffiths et al., 2002; Francke et al., 2013) showing the calculated local evaporation line (LEL) and global meteoric water line (GMWL), and (B) showing $\delta^{18}O$ and $\delta^{13}C_{DIC}$ of lake water and spring inflows (Griffiths et al., 2002; Francke et al., 2013).

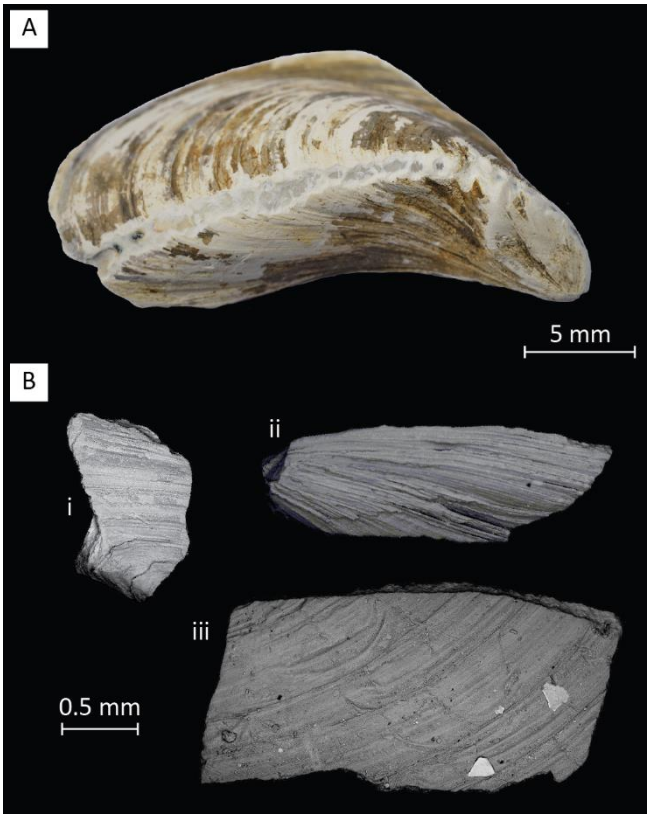

Figure 3 A) Modern whole shell collected from the littoral zone of Lake Dojran in June 2011 (scale bar = 5 mm), and B) shell fragments from 129 cm (i, ii) and 141 cm (iii) core depth (scale bar = 0.5 mm).

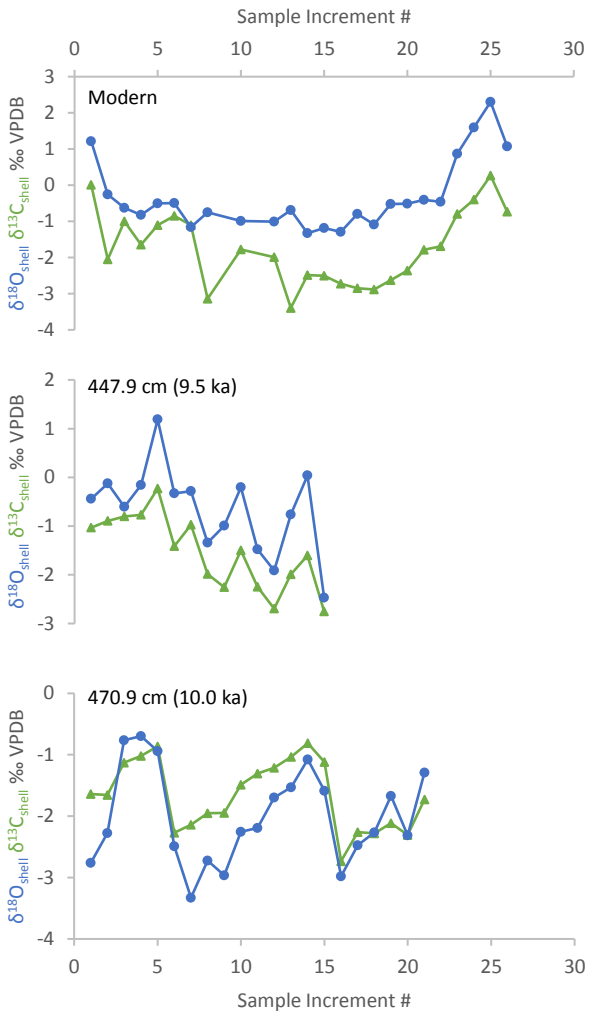

Figure 4 $\delta^{18}O$ (blue dots/lines) and $\delta^{13}C$ (green triangles/lines) from modern and fossil whole shells. Fossil shells were recovered from core depths of 447.9 cm (9.5 cal kyr BP) and 470.9 cm (10.0 cal kyr BP).

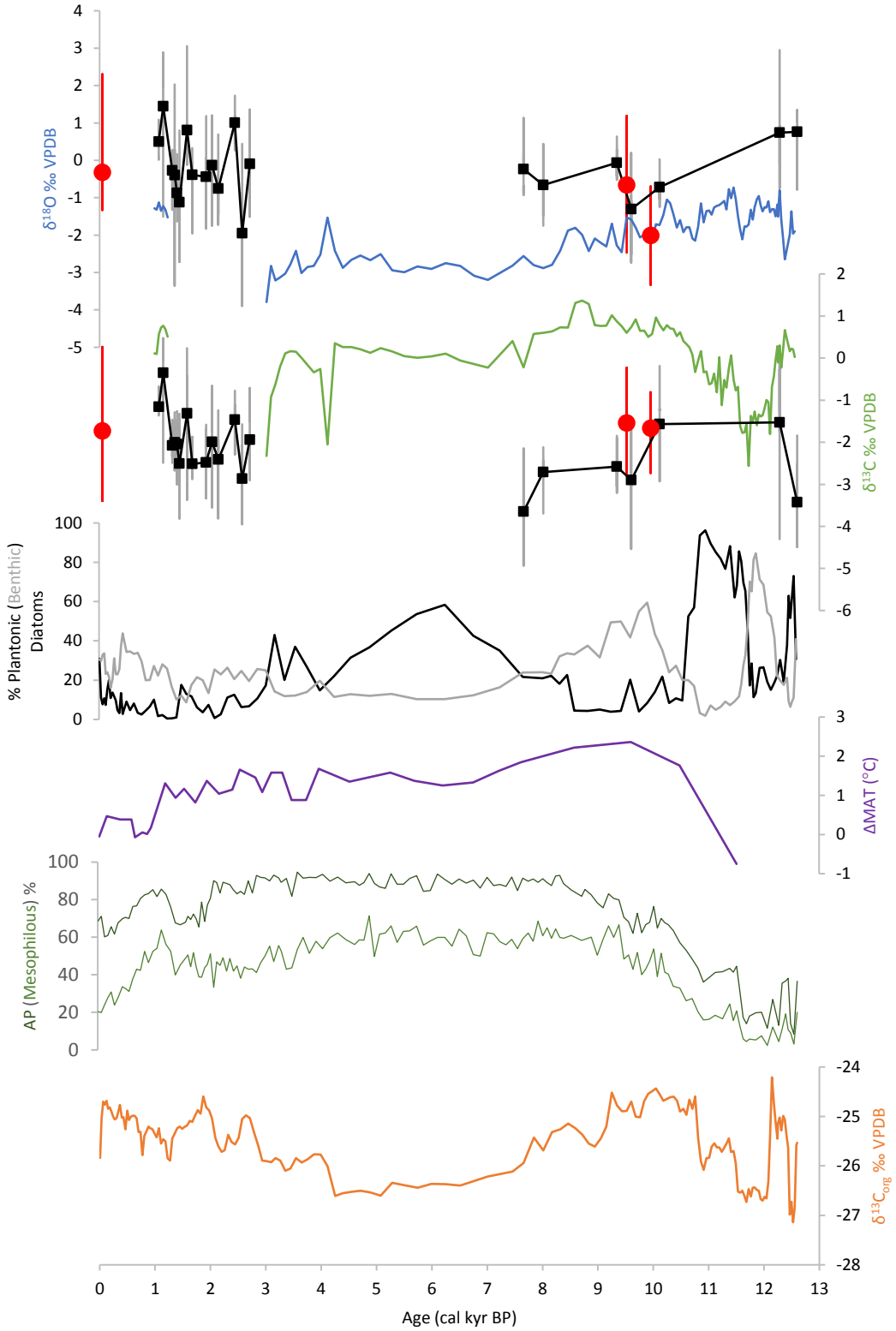

Figure 5 $\delta^{18}O$ and $\delta^{13}C$ from shell fragments (black square = average, black line = range), whole shells (red dot = average, red line = range), and endogenic inorganic carbonate (green and blue lines; Francke et al., 2013). A correction factor of +0.8 ‰ and +0.9 ‰ was applied to $\delta^{18}O_{carb}$ and $\delta^{13}C_{carb}$ (Rubinson & Clayton, 1969; Kim et al., 2007b), respectively, to report the endogenic carbonate (calcite) data as aragonite. Also shown are the relative abundance of planktonic and benthic diatoms (Zhang et al., 2014), relative annual mean air temperature change (Thienemann et al., 2017), percentage of arboreal pollen (AP) and mesophilous taxa (for taxa list see Masi et al., 2017), and the $\delta^{13}C$ of organic matter (Francke et al., 2013).